American Journal of Pathology, Vol. 164, No. 3, March 2004

Impaired Calcification Around Matrix Vesicles of Growth Plate and Bone in Alkaline Phosphatase-Deficient Mice

H. Clarke Anderson,* Joseph B. Sipe,* Lovisa Hessle,† Rama Dhamyamraju,* Elisa Atti,‡ Nancy P. Camacho,‡ and José Luis Millán†

From the Department of Pathology and Laboratory Medicine, University of Kansas Medical Center, Kansas City, Kansas; The Burnham Institute,† La Jolla, California; and the Hospital for Special Surgery,‡ New York, New York*

The presence of skeletal hypomineralization was confirmed in mice lacking the gene for bone alkaline phosphatase, ie, the tissue-non-specific isozyme of alkaline phosphatase (TNAP). In this study, a detailed characterization of the ultrastructural localization, the relative amount and ultrastructural morphology of bone mineral was carried out in tibial growth plates and in subjacent metaphyseal bone of 10-day-old TNAP knockout mice. Alizarin red staining, microcomputerized tomography (micro CT), and FTIR imaging spectroscopy (FT-IRIS) confirmed a significant overall decrease of mineral density in the cartilage and bone matrix of TNAP-deficient mice. Transmission electron microscopy (TEM) showed diminished mineral in growth plate cartilage and in newly formed bone matrix. High resolution TEM indicated that mineral crystals were initiated, as is normal, within matrix vesicles (MVs) of the growth plate and bone of TNAP-deficient mice. However, mineral crystal proliferation and growth was inhibited in the matrix surrounding MVs, as is the case in the hereditary human disease hypophosphatasia. These data suggest that hypomineralization in TNAP-deficient mice results primarily from an inability of initial mineral crystals within MVs to self-nucleate and to proliferate beyond the protective confines of the MV membrane. This failure of the second stage of mineral formation may be caused by an excess of the mineral inhibitor pyrophosphate (PPi) in the extracellular fluid around MVs. In normal circumstances, PPi is hydrolyzed by the TNAP of MVs' outer membrane yielding monophosphate ions (Pi) for incorporation into bone mineral. Thus, with TNAP deficiency a buildup of mineral-inhibiting PPi would be expected at the perimeter of MVs. *(Am J Pathol 2004, 164:841–847)*

In humans, a hereditary deficiency of the gene for tissue non-specific alkaline phosphatase (TNAP) leads to skeletal hypomineralization, reflected clinically as rickets and osteomalacia.[1–5] Also, there is increasing experimental evidence to indicate that skeletal alkaline phosphatase promotes *in vivo* biomineralization of normal growth plates, bones, and dentin.[6–11] Although the precise role of alkaline phosphatase in promoting mineralization has long been debated,[9] the balance of experimental evidence clearly indicates that the catalytic activity of alkaline phosphatase is required for normal skeletal calcification.[6,10,11]

The hypothesis that TNAP promotes skeletal mineralization *in vivo* also has been strengthened by the recent development of knockout mice lacking a functional TNAP gene.[12–14] The latter enzyme is highly expressed in normal bone, and also in liver and kidney.[15] TNAP knockout mice exhibit skeletal hypomineralization similar to that seen in patients with hypophosphatasia.[1,12–14] The question of whether hypomineralization in hypophosphatasia is due to a failure of mineral crystal initiation by extracellular matrix vesicles (MVs) has not yet been investigated in growth plates or bone of TNAP-deficient mice at the ultrastructural level.

Matrix vesicles (MVs) are alkaline phosphatase enriched,[8,16–19] submicroscopic, extracellular, membrane-invested bodies within which the first crystals of hydroxyapatite bone mineral are generated during normal mineral initiation in growth plate cartilage,[17] developing bone,[18] and dentin.[19] MVs are highly enriched in phosphatases, especially TNAP, ATPase, AMPase, inorganic pyrophosphatase, and nucleoside triphosphate pyrophosphohydrolase, also called NTPPase, NPP1, or PC-1.[16,20–23] TNAP and ATPase are bound to matrix vesicles' outer surfaces,[8,20] while the specific ultrastructural localization of inorganic PPiase has not yet been determined. There is considerable experimental evidence indicating that TNAP and ATPase can stimulate mineral deposition

Supported by National Institutes of Health Grants DE05262, CA42595, and DE12889.

Accepted for publication November 11, 2003.

Address reprint requests to H. Clarke Anderson, M.D., Department of Pathology and Laboratory Medicine, University of Kansas Medical Center, 3901 Rainbow Blvd., Kansas City, KS 66160. E-mail: handerso@kumc.edu.

in vitro by preparations of isolated MVs[21,23] or in slices of rachitic rat growth plate.[6]

In cases of hypophosphatasia, there is a hereditary deficiency of the TNAP gene.[2,3,5] MVs of the growth plate and metaphyseal bone of hypophosphatasia patients retain their ability to initiate intravesicular mineral.[1] In human hypophosphatasia, the failure of bones to calcify appears to result from a block in the vectorial spread of mineral, from initial crystal nuclei which form normally within MVs, outwards beyond the MV membrane and into the surrounding collagenous matrix.[1]

The objectives of the present study were to confirm earlier reports of a deficiency of mineralization in bones of TNAP knockout mice using more sensitive methods to measure the amount and distribution of mineral, including alizarin red stains of sections of epoxy resin-embedded upper tibias, Fourier transform infrared imaging spectroscopic (FT-IRIS) analysis of mineralization, and to quantitate bone mineral density by microCT, and to evaluate the ultrastructure of MVs in TNAP knockout mouse bones to confirm that hypomineralization results from a block of mineral propagation from MVs into the extracellular matrix, as occurs in human hypophosphatasia.

Materials and Methods

TNAP Knockout Mice

The generation of TNAP null mice has been previously reported.[13–15,24–26] The TNAP knockout mice used in this study were hybrids of C57Bl/6X129J mouse strains. TNAP−/− and +/− mutant mice show no apparent or radiographical skeletal abnormality at birth. However, during the first 10 postnatal days of age, TNAP−/− mice display impaired skeletal mineralization by X-ray.[13] After 10 to 14 days of age the TNAP knockout mice develop seizures, due to impaired utilization of pyridoxal phosphate (vitamin B6), and die.[25,26] Although pyridoxal phosphate can serve as a naturally occurring substrate for TNAP, its action as a vitamin is required for normal brain and central nervous system function.[25,26] In this study, 10-day-old TNAP−/− mice were used before they developed seizures and died.

Microcomputerized Tomography (MicroCT)

The distribution and relative density of bone mineral was imaged and measured by microCT, carried out by Enhanced Vision Systems Corporation (now GE Medical Systems) of London, Ontario, Canada. Specimens for microCT analysis consisted of sagitally-sectioned, 2.5% paraformaldehyde-fixed[17] upper tibias and attached femurs, dissected free of soft tissue. Volume cone-beam CT imaging was used to create 14 μm resolution volume data sets from four 10-day-old TNAP−/− mice and seven TNAP-wild-type (WT) mice. The microCT images were analyzed for bone volume fraction (BVF), reported as % of total bone volume, bone mineral density (BMD) in mg/ml, mean trabecular bone thickness (Tb.Th) in mm, and trabecular number (Tb. N) per mm^2 of bone surface.

Light Microscopy and Alizarin Red Calcium Stains

Non-decalcified upper tibial growth plates and subjacent metaphyseal and cortical bone were fixed in 2.5% glutaraldehyde, buffered with cacodylate[17] and then embedded in Spurr epoxy resin (Sigma, St. Louis, MO). Standard light microscopy was carried out on 1-μm thick sections of the Spurr-embedded bones after staining with toluidine blue. One-μm thick Spurr-embedded sections also were stained for calcium, using the alizarin red method of Gilmore et al,[27] which specifically stains calcium red in 1-μm bone sections without prior deplastization to remove the epoxy resin.

Fourier Transform Infrared Imaging Spectroscopy (FT-IRIS)

FT-IRIS was performed on 1-μm thick unstained Spurr-embedded sections from the same blocks used for light microscopy and alizarin red staining. Sections were cut onto BaF_2 infrared windows and a BioRad (Cambridge, MA) FTS-60A step-scanning Stingray 6000 FTIR spectrometer with a UMA 300A FTIR microscope (Biorad, Cambridge, MA) and a 64 × 64 MCT FPA detector was used to acquire spectra at 8 cm^{-1} resolution under N_2 purge. Data were collected from 400 × 400 μm^2 regions at 64 × 64 individual points of 7-μm diameter, resulting in 4096 individual spectra. Infrared vibrations of both the mineral and matrix phases were monitored simultaneously. The ratio of the area of the mineral phosphate n_1, ν_3 absorbance from 900 to 1200 cm^{-1} to the area of the protein amide I absorbance from 1590 to 1720 cm^{-1} was calculated to obtain the relative amounts of mineral and protein present (min:matrix). The ratio of the intensities of the phosphate contour at 1030 and 1020 cm^{-1} was calculated as an indicator of crystallinity. IR images were then created based on min:matrix and crystallinity.

Transmission Electron Microscopy

Ultra-thin sections were taken from the same sectioned surfaces of Spurr-embedded blocks of upper tibial growth plates and metaphysis that had been used to produce 1-μm thick sections for light microscopy and alizarin red staining. Transmission electron microscopy (TEM) sections were stained with lead citrate and uranyl acetate as previously described.[17] The sections were examined and photographed using a Zeiss EM10A electron microscope (Carl Zeiss, New York, NY).

Results

MicroCT (GE Medical Systems, London, Ontario, Canada) and alizarin red stains confirmed a reduced mineral content in TNAP knockout tibias. MicroCT images showed reduced mineralization of TNAP-deficient growth plates and metaphyses (Figure 1). Also, the epiphyses, ie, secondary ossification centers, were either absent or greatly reduced in

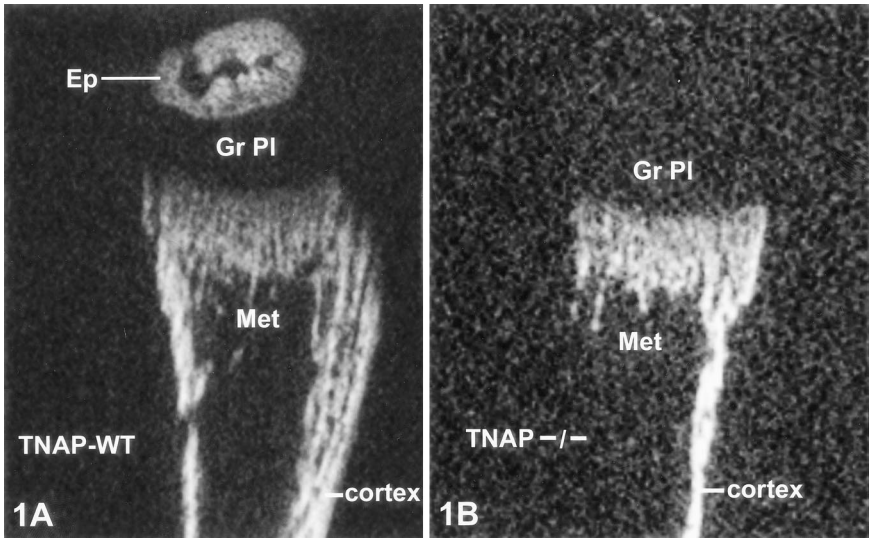

Figure 1. Micro-CT images of upper tibias from WT (**A**) and TNAP−/− (**B**) mice. Overall, mineral content was reduced in TNAP−/− mice, mineralized cortex was thinner, and epiphyses (Ep) were often not visible. Ep, epiphysis; GrPI, growth plate; Met, metaphysis.

TNAP deficiency (Figure 1B). Bone mineral density (BMD), bone volume fraction (BVF), and average bone trabecular thickness, as measured by microCT densitometry, were significantly reduced (Table 1). Alizarin red stains (Figure 2) showed a consistent decrease in the amount of calcification in lower, hypertrophic zones of growth plate as well as in metaphyseal bone trabeculae and cortical bone of TNAP knockout mice (Figure 2). In growth plates, mineral deposits that normally extend upward from the metaphysis, rose to a higher level in TNAP wild-type than in TNAP knockout tibias (Figure 2, B *versus* F). Also, there was an abnormal accumulation of uncalcified bone matrix (osteoid) at the surfaces of bone trabeculae in the metaphyses of TNAP-deficient mice (Figure 2, C *versus* G). The height of hypertrophic cartilage cell columns was slightly more variable in TNAP-deficient growth plates, ie, 11 to 21 cells per cell column in TNAP deficiency (mean, 14.7 ± 2.8 SE) *versus* a range of 12 to 19 cells per cell column in wild-type (mean, 14.3 ± 2.3 SE). However, the mean height of hypertrophic zones did not differ significantly between the two genotypes.

Similar to the Alizarin red stain and the microCT data, FT-IRIS images showed reduced mineralization (min:matrix) in the TNAP-knockout mice compared to wild-type mice (Figure 3A). This was apparent in both growth plate calcified cartilage and in metaphyseal trabecular bone. No differences in crystallinity of the mineral phase was detected (Figure 3B).

Table 1. Micro-CT Comparison of Average Bone Mineral Density (BMD), Bone Volume Fraction (BVF), and Trabecular Thickness in TNAP Wild-Type *versus* TNAP-Deficient Upper Tibias

Genotype	BMD (mg/cc)	BVF (%)	Trabecular thickness (mm)	*N*
TNAP WT	174 ± 38	45 ± 13	53 ± 21	7
TNAP$^{-/-}$	92 ± 8	27 ± 5	30 ± 6	4
P	0.002	0.03	0.06	

Data presented as means ± SD.

Transmission EM also showed a significant decrease of calcification in growth plates of TNAP knockout mice (Figure 4,A and B *versus* C and D). However, needle-like crystallites of apatitic mineral were present within MVs of both TNAP wild-type and deficient cartilage during early stages of mineralization (Figure 4, A *versus* C). At calcification sites near the junction of growth plate with metaphysis, where matrix calcification is normally advanced, the size and number of extravesicular mineral deposits was conspicuously reduced in TNAP-deficient growth plates (Figure 4, B *versus* D). Also, the needle-like deposits of electron dense mineral appeared fragmented and more granular in TNAP knockout mice than in wild-type mice (Figure 4, B *versus* D).

Surfaces of bone trabeculae in the metaphyses of TNAP knockout tibias showed a marked increase in residual, non-calcified bone matrix (osteoid) (Figure 5,A *versus* B). This increase in uncalcified bone matrix appeared in transmission EM as an abnormally thick accumulation of non-calcified, wide-diameter collagen fibrils (consistent with type I collagen), separating osteoblasts from the outer edges of mineralized matrix in TNAP-deficient mice (Figure 5B). Heavily calcified MVs were more numerous and conspicuous within the hypocalcified TNAP-deficient bone matrix (Figure 5B), but were also detected occasionally in thin seams of osteoid at the surfaces of normal bone trabeculae (Figure 5A).

Discussion

Our present findings in TNAP knockout mice are consistent with earlier reports indicating a significant hypomineralization of growth plates and bones in human patients with hereditary hypophosphatasia.[1–3,5] Also, a dependence of skeletal mineralization on alkaline phosphatase enzymatic activity has been reported in mice whose bones are genetically deficient in tissue-non-specific alkaline phosphatase (TNAP).[12–14] Thus, there is consider-

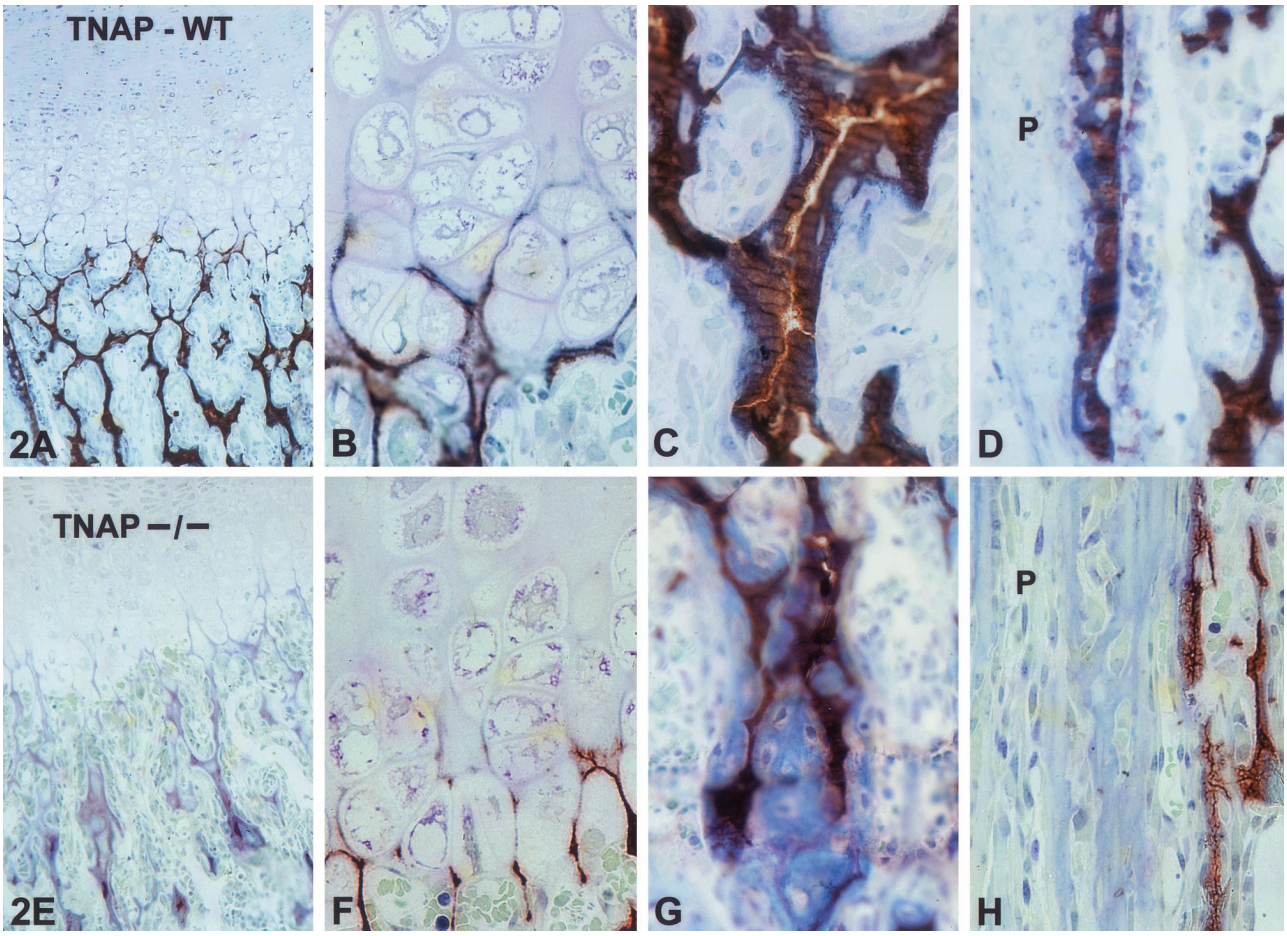

Figure 2. Alizarin red calcium stains for mineral in TNAP WT growth plate (**A** and **B**), metaphysis (**C**) and cortex (**D**) *versus* TNAP-deficient growth plate (**E** and **F**), metaphysis (**G**) and cortex (**H**). TNAP-deficient tibias showed respectively a significant reduction in alizarin-stained mineral in growth plate, metaphysis (where in TNAP deficiency there was an excess of blue-staining osteoid bone matrix), and in cortex. **A**, magnification × 280; **E**, magnification × 354; **B–D** and **F–H**, magnification × 1100.

able evidence indicating that the catalytic activity of TNAP is an important promoter of bone mineralization *in vivo*.

Two major hypotheses have been advanced to explain how alkaline phosphatase (TNAP) could promote biomineralization. First, it was proposed by Robison[9] in the 1920's that alkaline phosphatase in bone hydrolyzes organic phosphate esters (eg, AMP or inorganic PPi), thus generating orthophosphate (Pi) for incorporation into nascent calcium phosphate mineral. This hypothesis is

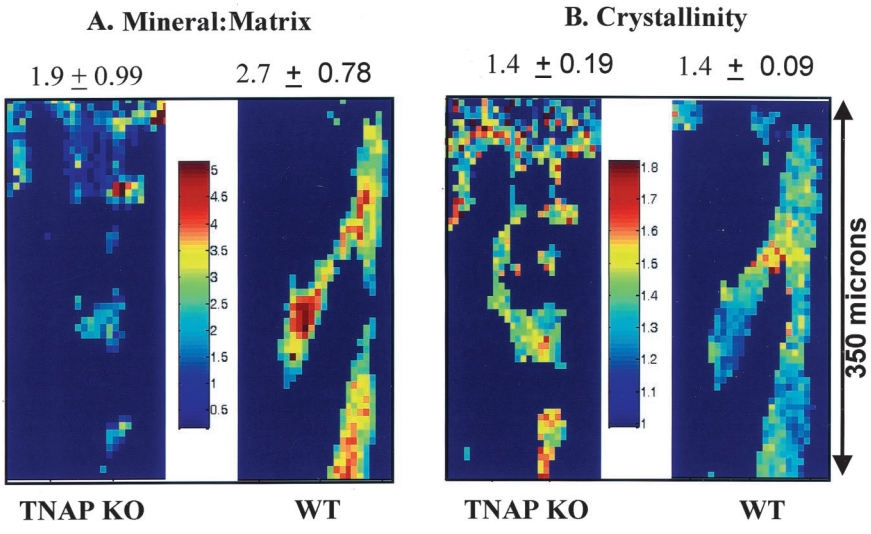

Figure 3. FT-IRIS images of TNAP WT *versus* TNAP-deficient growth plate and metaphysis. The mineral:matrix (**A**) was calculated from the ratio of the area of phosphate 900-1200 cm^{-1} absorbance to the area of the protein amide I absorbance from 1590 to 1720 $cm^{[minus1}$. The distribution of the crystallinity (**B**) of the mineral phase was calculated by establishing the ratio of the intensity of the absorbance at 1030 cm^{-1} to that at 1020 cm^{-1}. Means ± standard deviations are shown for each value.

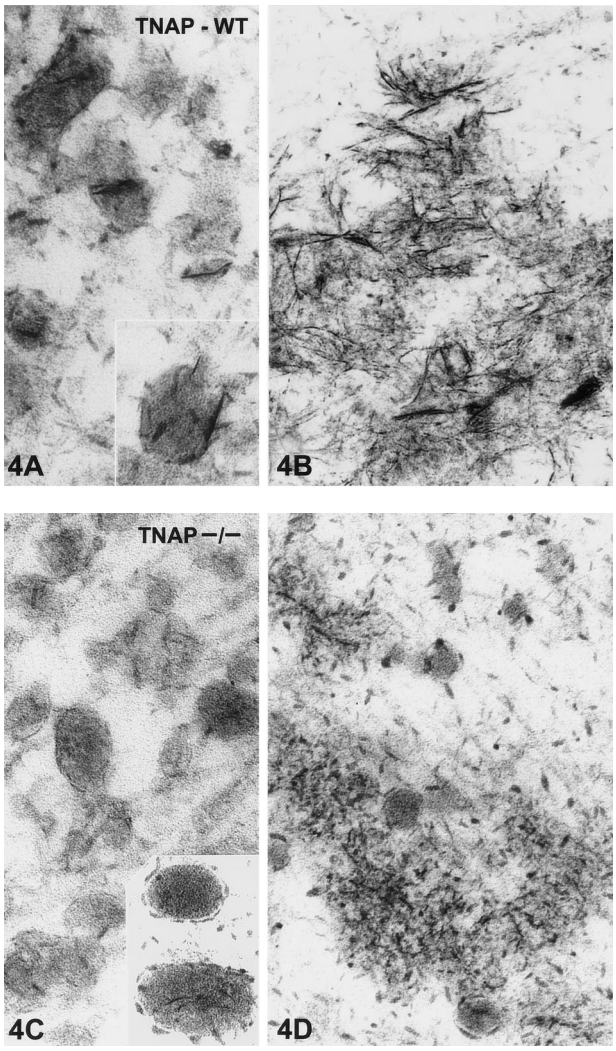

Figure 4. Transmission electron micrographs of TNAP WT *versus* TNAP-deficient growth plates (**A** *versus* **C**) at the onset of mineralization. In the upper growth plate, (**A** *versus* **C**), needle-like crystallites of apatitic mineral were present in both WT and TNAP-deficient MVs, although mineral crystallites were more prominent in WT. At the junction between growth plate and metaphysis (**B** and **D**), the size and number of extravesicular mineral deposits in cartilage matrix was reduced in TNAP-deficient animals (**D**) *versus* WT (**B**), and often TNAP-deficient mineral appeared fragmented and more granular (**D**). Small, leaf-like, electron-dense proteoglycan granules are seen in the background cartilage matrix where they are attached to randomly arranged, faintly visible type II collagen fibrils. **A** and **D**, magnification × 115,000; **B**, magnification × 71,000; **C**, magnification × 150,000.

supported by recent *in vitro* experiments showing that alkaline phosphatase hydrolysis of ester phosphate substrates such as β-glycerophosphate can stimulate the initiation and propagation of mineralization by cultured bone or cartilage cells[10,11] or by isolated growth plate MVs.[21] Furthermore, *in vitro* cartilage calcification was inhibited by L-tetramisole,[11] which is a relatively specific inhibitor of TNAP catalytic activity.

The second major hypothesis, advanced to explain alkaline phosphatase promotion of skeletal mineralization, proposes that the main function of TNAP is to hydrolyze inorganic pyrophosphate (PPi) at the site of mineral crystal proliferation.[28,29] Pyrophosphate is normally generated during the hydrolysis of ATP by nucleoside triphosphate pyrophosphohydrolase (NTPPase, also known as PC-1) (see diagram in Figure 6). NTPPase is concentrated in MVs.[8,16] Above normal levels of PPi have been shown to inhibit mineral propagation *in vitro*[28,29]. In hypophosphatasia, excess PPi accumulation at sites of nascent calcification, resulting from insufficient hydrolysis of PPi in TNAP-deficient bone, would tend to bind to the surfaces of preformed crystals of hydroxyapatite, thus preventing crystal proliferation.[30] The simultaneous deletion of the TNAP and PC-1 genes leads to normalization of the PPi levels in MVs.[31]

When considered in the context of matrix vesicles, which generate the first crystals of hydroxyapatite within the protective confines of their membranes,[17,19] the first hypothesis above would seem to predict a failure of initial mineralization within MVs in TNAP deficiency, while the second hypothesis would predict a failure of mineral propagation beyond the MVs and out into the surrounding collagenous matrix. Clearly, a combination of the above two hypothetical mechanisms could be operative and thus lead to defective mineralization in TNAP-deficient mice. Not only could insufficient TNAP catalytic activity fail to hydrolyze PPi, thus limiting the amount of Pi available to support initial mineral formation, but the resulting build-up of unhydrolyzed PPi in the perivesicular matrix could inhibit the proliferation of pre-formed HA crystals, outwards, beyond the protective confines of the MV membranes (Figure 5). The balance of evidence from this and earlier studies would seem to suggest primarily a failure of mineral propagation, due to excessive build-up of PPi,[28–31] as the main cause of the hypomineralization seen in human hypophosphatasia and in TNAP knockout mice.[31]

However, matrix vesicles that are deficient in TNAP may yet be capable of initiating intravesicular mineralization through the compensatory activity of other phosphatases that are known to be concentrated in MVs (eg, AMPase and/or inorganic pyrophosphatase).[16] Even in the absence of TNAP these phosphatases could hydrolyze PPi and other substrates (eg, AMP), thus supplying Pi for incorporation into initial mineral within MVs,[32] but still be insufficient to remove excess PPi at the perimeter of MVs. Thus, despite TNAP deficiency, initial mineral could form within MVs, while its propagation into the perivesicular matrix would be hindered by a local build-up of PPi. At a distance from MVs in the matrix, the abnormally high perivesicular levels of PPi, resulting from TNAP deficiency in MVs, probably would be diluted out by extracellular fluid, which normally contains a very low concentration of PPi (approximately 0.1 to 1.0 micromolar).[33] Thus, mineral crystal formation could resume at a sufficient distance from MVs as observed. Our present finding in TNAP deficiency of a wide band of unmineralized cartilage and bone matrix between MVs and zones of matrix calcification would seem to support the hypothesis that high PPi at the perimeter of TNAP-deficient MVs is preventing crystal growth in this localized region of the matrix.

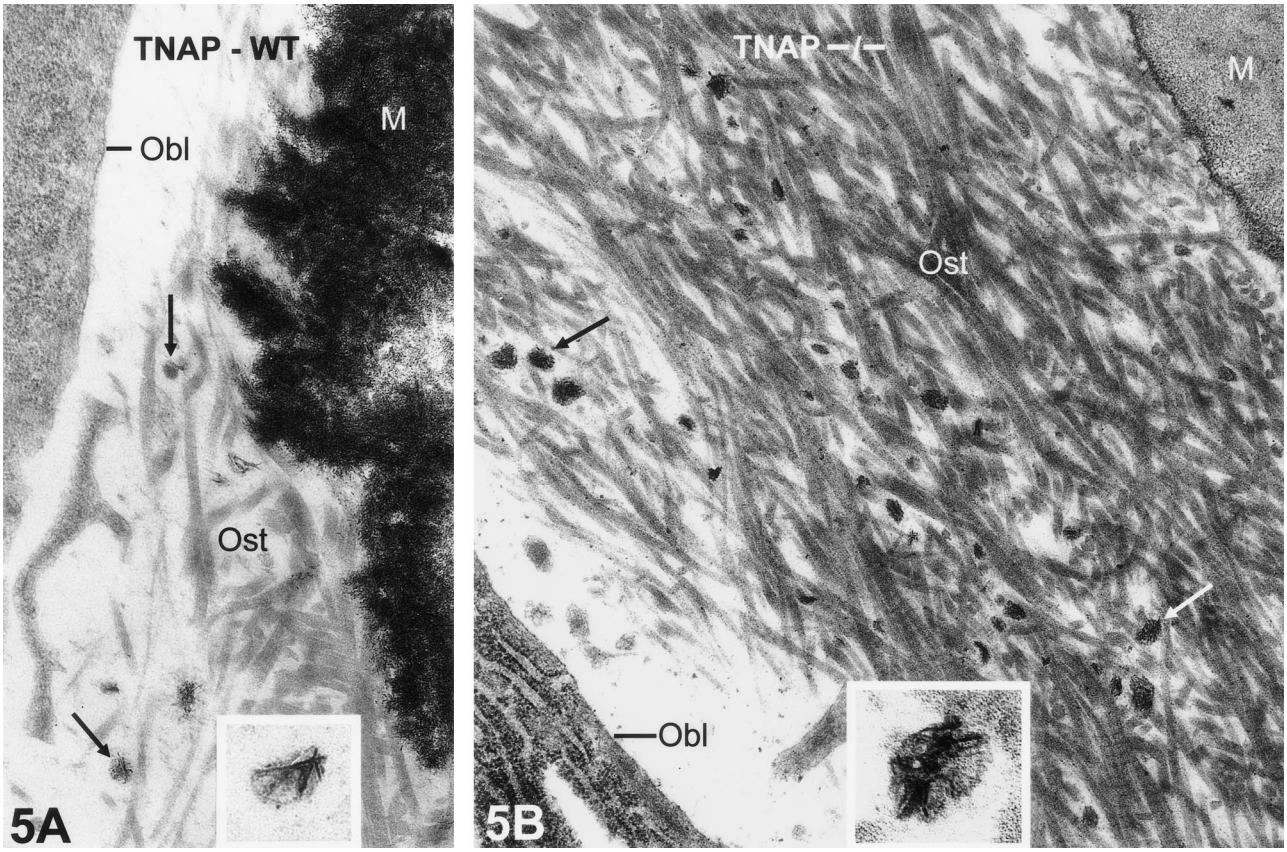

Figure 5. Normal uncalcified osteoid (Ost) layer (**A**) *versus* widened osteoid layer in TNAP-deficient tibial metaphyseal bone (**B**). A few intact matrix vesicles, containing apatite-like needles (indicated by **arrows** and shown at higher magnification in inserts, are present in the uncalcified osteoid of both TNAP wild-type and TNAP-deficient tibias. M, mineralized bone matrix; Obl, osteoblast; Ost, osteoid. **A** and **B**, magnification × 25,000; **A inset**, magnification × 61,000; **B inset**, magnification × 127,000.

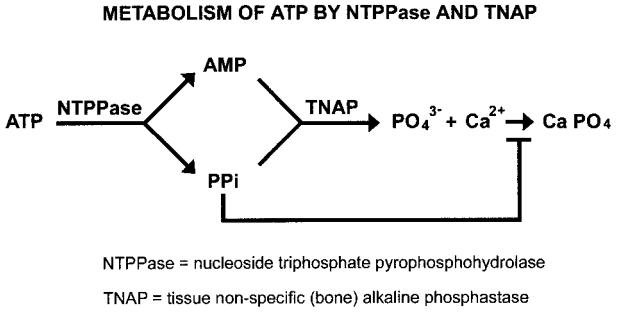

Figure 6. Diagram outlining the metabolic sequence that occurs when ATP is hydrolyzed by nucleoside triphosphate pyrophosphohydrolase (NTPPase, also known as PC-1). Following ATP hydrolysis by NTPPase to adenosine monophosphate (AMP) plus inorganic pyrophosphate (PPi), both of these ester phosphates are further hydrolyzed to orthophosphate (PO_4^{3-}) by alkaline phosphatase (TNAP). The resulting orthophosphate molecules are incorporated into calcium phosphate mineral. Abnormally high levels of non-hydrolyzed PPi block the formation of calcium phosphate mineral.[28,29]

References

1. Anderson HC, Hsu HHT, Morris DC, Fedde KN, Whyte MP: Matrix vesicles in osteomalacic hypophosphatasia bone contain apatite-like mineral crystals. Am J Pathol 1997, 151:1555–1561
2. Henthorn PS, Reduchov M, Fedde KN, Lafferty MA, Whyte MD: Different missense mutations at the tissue-non-specific alkaline phosphatase gene locus in autosomal recessively inherited forms of mild and severe hypoplasia. Proc Nat Acad Sci USA 1992, 89:9924–9928
3. McCance RA, Fairweather DV, Barrett AM, Morrison AB: Genetic, clinical, biochemical, and pathological features of hypophosphatasia. Q J Med 1956, 25:523–538
4. Wennberg C, Hessle L, Lundberg P, Mauro S, Narisawa S, Lerner VH, Millan JL: Functional characterization of osteoblasts and osteoclasts from alkaline phosphatase knockout mice. J Bone Miner Res 2000, 15:1879–1888
5. Whyte MP: Hypophosphatasia. Metabolic and Molecular Bases of Inherited Disease, ed 8. Edited by Schriver CL, Beaudet AL, Sly WS, Valle D, Childs B, Kinzler KW, Vogelstein B. New York, McGraw Hill, 2000, pp 5313–5329
6. Anderson HC, Sajdera SW: Calcification of rachitic cartilage to study matrix vesicle function. Fed Proc 1976, 35:148–153
7. Johnson TF, Morris DC, Anderson HC: Matrix vesicles and calcification of rachitic rat osteoid. J Exp Pathol 1989, 4:123–132
8. Matsuzawa T, Anderson HC: Phosphatases of epiphyseal cartilage studied by electron microscopic cytochemical methods. J Histochem Cytochem 1971, 19:801–808
9. Robison R: The possible significance of hexosephosphoric esters in ossification: a reply to Shipley, Kramer, and Howland. Biochem J 1926, 20:388–391
10. Bellows CG, Aubin JE, Heersch JNM: Initiation and progression of mineralization of bone nodules formed in vitro: the role of alkaline phosphatase and organic phosphate. Bone Miner 1991, 14:27–40
11. Fallon MD, Whyte MP, Teitlebaum SL: Stereospecific inhibition of alkaline phosphatase by L-tetramisole prevents in vitro cartilage calcification. Lab Invest 1980, 43:489–494
12. Fedde KN, Blair L, Silverstein J, Coburn SP, Ryan LM, Weinstein RS, Waymine K, Narisawa S, Millan J, McGregor GR, Whyte MP: Alkaline phosphatase knockout mice recapitulate the metabolic and skeletal defects of infantile hypophosphatasia. J Bone Miner Res 1999, 14: 2015–2026
13. Narisawa S, Frohlander N, Millan JL: Inactivation of two mouse alka-

line phosphatase genes and establishment of a model of infantile hypophosphatasia. Dev Dyn 1997, 208:432–446
14. Tesch W, Vandenbos T, Roschgr P, Fratze-Zelman N, Klaushofer K, Beertsen W, Fratzl P: Orientation of mineral crystallites and mineral density during skeletal development in mice deficient in tissue nonspecific alkaline phosphatase. J Bone Miner Res 2003, 18:117–125
15. Weiss MJ, Ray F, Fallon MD, Whyte MP, Fedde KN, Lafferty MA, Mulivor RA, Harris H: Analysis of liver, bone, and kidney alkaline phosphatase messenger-RNA, DNA, and enzymatic activity in cultured skin fibroblasts from 14 unrelated patients with severe hypophosphatasia. Am J Hum Genet 1989, 44:686–694
16. Ali SY, Sajdera SW, Anderson HC: Isolation and characterization of calcifying matrix vesicles from epiphyseal cartilage. Proc Natl Acad Sci USA 1970, 67:1513–1520
17. Anderson HC: Vesicles associated with calcification in the matrix of epiphyseal cartilage. J Cell Biol 1969, 41:59–72
18. Anderson HC, Reynolds JR: Pyrophosphate stimulation of calcium uptake into cultured embryonic bones: fine structure of matrix vesicles and their role in calcification. Dev Biol 1973, 34:211–227
19. Anderson HC: Molecular biology of matrix vesicles. Clin Orthop Relat Res 1995, 314:266–280
20. Akisaka T, Gay CV: Ultrastructural localization of calcium-activated adenosine triphosphatase (Ca+-ATPase) in growth plate cartilage. J Histochem Cytochem 1985, 33:925–932
21. Ali SY, Evans L: The uptake of [^{45}Ca] calcium ions by matrix vesicles isolated from calcifying cartilage. Biochem J 1973, 134:647–650
22. Hsu HHT: Purification and partial characterization of ATP-pyrophosphohydrolase from fetal bovine epiphyseal cartilage. J Biol Chem 1983, 258:3463–3464
23. Hsu HHT, Anderson HC: Evidence of the presence of a specific ATPase responsible for ATP-initiated calcification by matrix vesicles isolated from cartilage and bone. J Biol Chem 1996, 271:26383–26388
24. MacGregor GR, Zambrowicz BP, Soriano P: Tissue non-specific alkaline phosphatase is expressed in both embryonic and extra-embryonic lineages during mouse embryogenesis but it is not required for migration of primordial germ cells. Development 1995, 121:1487–1496
25. Waymire KG, Mahurin JD, Jaje JM, Guilarte TR, Coburn SP, McGregor GR: Mice lacking tissue non-specific alkaline phosphatase die from seizures due to defective metabolism of vitamin B-6. Nat Genet 1995, 11:45–51
26. Narisawa S, Wennberg C, Millan JL: Abnormal vitamin B-6 metabolism in alkaline phosphatase knock-out mice causes multiple abnormalities but not the impaired bone mineralization. J Pathol 2001, 193:125–133
27. Gilmore S, Whitson SW, Bowers DE: A simple method using alizarin red-S for the detection of calcium in epoxy-resin embedded tissue. Stain Technol 1986, 61:89–92
28. Fleisch H, Straumann F, Schenk R, Bizaz S, Allgower M: Effect of condensed phosphates on calcification of chick embryo femurs in tissue culture. Am J Physiol 1966, 211:821–825
29. Russell RG, Bisaz S, Donath A, Morgan DB, Fleisch H: Inorganic pyrophosphate in plasma in normal persons and in patients with hypophosphatasia, osteogenesis imperfecta, and other disorders of bone. J Clin Invest 1971, 50: 961–969
30. Termine JD, Conn KM: Inhibition of apatite formation by phosphorylated metabolites and macromolecules. Calcif Tissue Res 1976, 22: 149–157
31. Hessle L, Johnson KA, Anderson HC, Narisawa S, Sali A, Gooding JW, Terkeltaub R, Millan JL: Tissue-non-specific alkaline phosphatase and plasma cell membrane glycoprotein-1 are central antagonistic regulators of bone mineralization. Proc Nat Acad Sci USA 2002, 99:9445–9449
32. Anderson HC, Reynolds JJ: Pyrophosphate stimulation of initial mineralization in cultured embryonic bones. Dev Biol 1973, 34: 211–227
33. Perkins HR, Walker PG: Occurrence of pyrophosphate in bone. J Bone Joint Surg 1958, 40:333–339